Plasma Medicine, 7(3):283–297 (2017)

Nanosecond-Pulsed Dielectric Barrier Discharge–Induced Antitumor Effects Propagate through Depth of Tissue via Intracellular Signaling

P. Ranieri, R. Shrivastav, M. Wang, A. Lin, G. Fridman, A. Fridman, L.-H. Han, & V. Miller*

Drexel University, C. & J. Nyheim, Camden, NJ 08103

*Address all correspondence to: Vandana Miller, Drexel University, C. & J. Nyheim, 200 Federal St., Suite 500, Camden, NJ 08103; Tel.: 215-571-4074; Fax: 215-895-1633, E-mail: vmiller@coe.drexel.edu

ABSTRACT: Studies using xenograft mouse models have shown that plasma applied to the skin overlying tumors results in tumor shrinkage. Plasma is considered a nonpenetrating treatment; however, these studies demonstrate plasma effects that occur beyond the postulated depth of physical penetration of plasma components. The present study examines the propagation of plasma effects through a tissue model using three-dimensional, cell-laden extracellular matrices (ECMs). These ECMs are used as barriers against direct plasma penetration. By placing them onto a monolayer of target cancer cells to create an *in-vitro* analog to *in-vivo* studies, we distinguished between cellular effects from direct plasma exposure and cellular effects due to cell-to-cell signaling stimulated by plasma. We show that nanosecond-pulsed dielectric barrier discharge plasma treatment applied atop an acellular barrier impedes the externalization of calreticulin (CRT) in the target cells. In contrast, when a barrier is populated with cells, CRT externalization is restored. Thus, we demonstrate that plasma components stimulate signaling among cells embedded in the barrier to transfer plasma effects to the target cells.

KEY WORDS: nanosecond-pulsed plasma, tumor cells, depth of penetration, calreticulin, cell signaling

I. INTRODUCTION

In the past decade, nonthermal plasma has emerged as a potential antitumor therapy due to its selectivity to adversely affect tumor cells compared to healthy cells.[1–4] Both *in-vitro* and *in-vivo* studies have demonstrated the efficacy of treatment with atmospheric pressure plasma jets (APPJ), dielectric barrier discharges (DBDs), and plasma-activated media (PAM).[5–9] For treatment of subcutaneous tumors *in vivo*, jets and DBDs generate plasma on the overlying skin, resulting in shrinkage of tumors one order of magnitude deeper than the theoretical penetration depth of plasma (1 mm vs 0.05 mm).[10,11] The mechanism by which plasma penetrates through this tissue to selectively affect the tumors underneath is unclear but critical to understand for clinical use of plasma.[4]

For the application of plasma-based therapy, the depth of penetration of treatment will determine whether the therapy is applicable to deep tumors as well. As shown in

1947-5764/17/$35.00

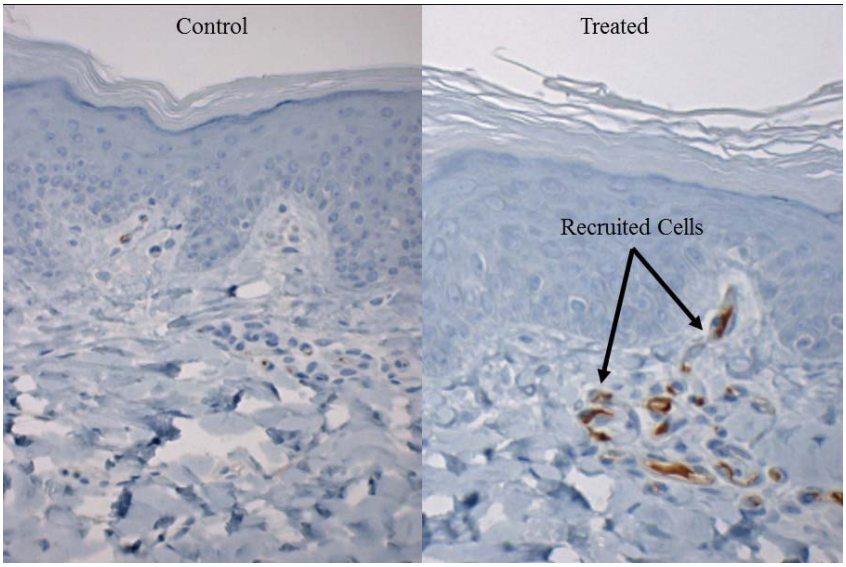

FIG. 1: nspDBD plasma induces recruitment of antigen-presenting cells in a pig model. Porcine skin was treated once at 9000 mJ. Biopsies were taken 1 wk after treatment and stained with CD163 antibody, targeting antigen-presenting cells of myeloid origin. Plasma treatment caused these cells to migrate to the treatment site from surrounding tissue.

Fig. 1, nspDBD treatment of porcine skin recruited immune cells to the treatment site. Both plasma-treated and untreated skin tissue were stained for CD163, an immune cell marker, 1 wk after plasma treatment. The presence of recruited cells beneath the skin shows evidence that plasma, widely considered a surface treatment modality, can interact with the surface tissue to affect cells deep into the tissue.[12]

A proposed pathway for cancer treatment using plasma is the stimulation of immune cells to target and eliminate tumors.[13] Although multiple approaches to immunotherapy exist, the uniqueness of plasma is its ability to noninvasively and simultaneously stimulate the immune cells while selectively stressing tumor cells.[14–16] Nanosecond-pulsed dielectric barrier discharge (nspDBD) plasma treatment has enhanced macrophage function directly.[17,18] It has also induced immunogenic cell death (ICD) in cancer cells *in vitro*. Additionally, in a coculture system, signals released from tumor cells undergoing ICD enhanced the efficacy of macrophages to eliminate the cancer cells.[14] This mechanism is even more selective, because stimulated immune cells will recognize and remove cancer cells but leave the healthy cells unaffected.[13]

Our recent *in-vivo* studies use nspDBD plasma for treatment of subcutaneous colorectal tumors through the proposed immunotherapy mechanism.[13,19] To determine how nspDBD plasma can penetrate the overlying tissue to induce ICD in the tumor, we modeled this system (Fig. 2) using collagen-based nanofibers to create a three-dimensional (3D) extracellular matrix (ECM) representing the tissue *in vitro*.[20] The tissue

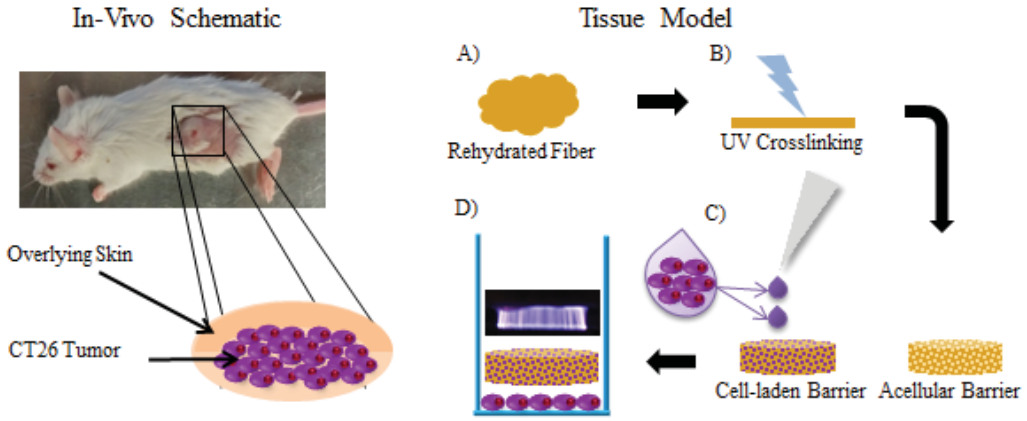

FIG. 2: Schematic of the fabrication process of the tissue model, which consists of rehydrating the freeze-dried fibers (A), molding into a sheet and photo–cross-linking using 365-nm UV light (B), punching out 10-mm diameter barriers using a biopsy punch and adding cells for the cell-laden barrier (C), and placing the barrier on a monolayer of cells (D). Cells added to the barrier grow until they are confluent before use.

model is placed on top of a monolayer of cancer cells, mimicking a tissue layer between plasma components and the tumor. NspDBD treatment was applied to the surface of the barrier and responses in the cancer cells below were measured.

II. MATERIALS AND METHODS

A. Cell Culture, Cells to Cells

Cell of the mouse colorectal cancer cell line CT26 (a gift from Dr. Adam Snook, department of pharmacology, Thomas Jefferson University, Philadelphia, PA) were grown in Dulbecco's Modified Eagle's Medium with glucose and sodium pyruvate (Corning Life Sciences, Tewksbury, MA) with 10% fetal bovine serum (FBS) (Corning Life Sciences, Tewksbury, MA) and 1% penicillin/streptomycin (P/S) (Life Technologies) and then incubated at 37ºC with 5% CO_2.

B. Tissue Model Fabrication and Culture

Freeze-dried, porcine, gelatin-based nanofibers (Sigma-Aldrich; St. Louis, MO) were fabricated in the lab of Dr. Li-Hsin Han, department of mechanical engineering and mechanics, Drexel University, Philadelphia, PA. The original method was tailored for fabrication of the tissue model with 10-mm-diameter fibers and 5–10-μm^2 pores.[20,21] The frozen nanofibers were mixed with a solution of PBS without Ca and Mg (Corning Life Sciences, Tewksbury, MA) and 0.05% lithium phenyl-2,4,6-trimethylben-

zoylphosphinate (LAP/BioKey, BioBots, Philadelphia, PA) (weight %) for 30 min at 37ºC to attach a cross-linking agent to the nanofibers. After rehydration, the fibers were minced to form a putty-like paste. To fabricate 150-µm sheets of nanofibers, the paste was loaded between two microscope slides with a No. 1 cover slip (ThermoFisher Scientific) for a 150-µm spacing, treated with ultraviolet (UV) light at 365 nm for 5 min, and immediately placed into 10 mL PBS without Ca and Mg. Barriers that are 10 mm in diameter are punched out from the sheets using a biopsy punch (fabricated at the Nyheim Plasma Institute, Drexel University) and placed into an individual well plate. These barriers were washed twice with 0.5 mL PBS without Ca and Mg. For an acellular ECM, the barrier is ready to use in the model. To prepare a cell-laden barrier, the PBS without Ca and Mg was removed, and 5.0E4 cells in 20 uL of media were slowly added atop the barrier and incubated for 25 min to allow cells to adhere to the barrier. Once attached, 0.5 mL media was added to the cell-laden barrier and incubated for 72 hr to reach 100% confluence.

C. nspDBD Plasma Treatment

Atmospheric pressure plasma was generated using an nsp power supply (FPB-20-05NM; FID GmbH; Burbach, Germany). As done in previous work, the pulser generated a 29-kV pulse with a rise time of 2 ns and pulse width of 20 ns.[14] A function generator (TG5011 LXI; TTI, Inc., Fort Worth, TX) was used to change the frequency between treatments. Each treatment had a fixed time and gap distance of 10 s and 1 mm, respectively. The energy per pulse for a 24-well plate was found to be 0.9 mJ/pulse.[14] One day before plasma treatment, CT26 cells were seeded in 24-well plates at 1.5e5 cells/well in 0.5-mL media and then incubated for 24 hr. To prepare the cells for plasma treatment, media were removed and the cells were washed with 0.5 mL PBS with Ca and Mg (Corning Life Sciences, Tewksbury, MA). The cells were treated with plasma by removing the PBS, applying the plasma at the 1-mm gap distance, and subsequently adding 0.5 mL media. When adding the barrier, both the acellular barrier and cell-laden barrier were washed twice with 0.5 mL PBS with Ca and Mg. Before treatment, PBS was removed from both the cells and barrier, and the barrier was lifted with forceps and placed gently in the center of the well on top of the cells. Plasma was generated 1 mm above the barrier, followed by the addition of 0.750 mL media. Both 2D and 3D plasma-treated cell cultures were incubated for 24 hr at 37ºC with 5% CO_2 following plasma treatment.

D. Extracellular ATP Measurement

Release of adenosine 5′-triphosphate (ATP) in response to nspDBD plasma treatment was measured as described previously.[14] Briefly, 0.05 mL media was collected 10 min after treatment and diluted with 0.1 mL UltraPure DNase/RNase-free distilled water (Thermo Fisher Scientific; Rochester, NY). To determine the concentration of extracellular ATP, the light generated during the chemical reaction between a bioluminescent

somatic cell assay kit (Sigma-Aldrich; St. Louis, MO) and ATP was measured using the PhotonMaster luminometer (PM10146; LuminUltra; New Brunswick, Canada). The ATP mix stock and buffer were combined to create a working solution that was then added to the media–water mixture. The relative light unit was measured immediately after adding the working solution.

E. Ecto-Calreticulin Measurement

Surface calreticulin (CRT) expression was determined using fluorescence staining through an image cytometer (Nexcelom Bioscience; Lawrence, MA). Cells were incubated for 24 hr after plasma treatment. The barriers were detached from the monolayer by slowly adding 2 mL PBS without Ca and Mg, until they were in suspension and were then removed with forceps. The barriers were set aside for fixation, and the target cells were collected and prepared for staining. Primary (PA3-900 CRT Polyclonal; Thermo Fisher Scientific; Rochester, NY) and secondary (A-11008; Goat Anti-Rabbit Alexa Fluor 488; Thermo Fisher Scientific; Rochester, NY) antibodies were used to stain for surface expression of CRT. Size and fluorescence intensity gating were done using FCS flow cytometry software (De Novo Software; Glendale, CA).

F. Fluorescence Imaging

The acellular and cell-laden barriers used in experiments were fixed using 4% paraformaldehyde (PFA) in PBS (PFA Affymetrix; Thermo Fisher Scientific; Rochester, NY) for 60 min. Fixed barriers were then washed twice by adding 0.5 mL PBS without Ca and Mg at 10-min intervals and stored in PBS without Ca and Mg. To process the sample for imaging, cells on the fixed barriers were permeabilized in 0.5 mL 0.2% Triton 100× in PBS without Ca and Mg for 30 min. After washing thrice in 10-min intervals with 2 mL PBS without Ca and Mg, the samples were blocked in 0.5 mL 2% bovine serum albumin and 0.2% Triton 100× in PBS without Ca and Mg and the incubated with agitation for 30 min. Samples were washed two more times in 10-min intervals and stained for nucleic acid using 400 pM of Hoechst stain (33258; Sigma-Aldrich; St. Louis, MO) for 10 min or the cellular cytoskeleton through F-actin filaments using 2 nM phalloidin-betramethylrhodamine B isothiocyanate (Sigma-Aldrich; St. Louis, MO) for 45 min. Once stained, samples were washed thrice at 10-min intervals. Before loading onto the microscope, the fixed barriers were compressed between two 1-mm microscope slides, similarly to the fabrication setup. Images were taken using confocal microscopy (SP5; Leica; Buffalo Grove, IL) at 20× magnification.

G. Statistical Analyses

Data were analyzed through one-way analysis of variance (ANOVA) parametric tests to assess the significance between treated and control samples (0 mJ). Treated samples were tested against the controls of similar experimental design, for example, treated

cell-laden barriers were compared with control cell-laden barriers. Samples are plotted using mean and standard deviation, with $n \geq 3$.

III. RESULTS AND DISCUSSION

A monolayer of CT26 cells was treated with nspDBD plasma in the presence or absence of a barrier to evaluate the depth of penetration of plasma treatment. The expression of ecto-CRT, a marker for the initiation of ICD, in the monolayer was used to indicate whether plasma effects reached the cells below the barrier.[22] Plasma interacts with cells in the barrier through the direct diffusion of plasma components (UV radiation, reactive oxygen and nitrogen species, electric field, and neutral species), induces oxidative stress, and stimulates redox-based signaling responses in both cancerous and healthy cells.[23,24] Plasma-generated reactive species have limited half-lives and diffusion distances, which are theorized to limit the depth of plasma treatment effect.[2] To distinguish between tumor cell responses to plasma components and to a combination of plasma-stimulated intercellular signaling and components, the barriers were acellular or loaded with cells, respectively.

A. nspDBD Plasma Treatment Induces Ecto-CRT Expression in CT26 Cancer Cells

A baseline of ecto-CRT expression in CT26 colorectal cancer cells was established in cells grown and treated in the absence of a barrier. Cells were collected 24 hr after plasma treatment and stained for CRT. Plasma treatment at 300 mJ increased the externalization of CRT on cells from 7.5% to 16.8% (Fig. 3A). This result, a twofold increase in the expression of ecto-CRT, compares to our previous studies at the same energy.[14] In subsequent studies, this served as a positive control to determine whether plasma treatment penetrated the tissue model to affect cells underneath.

B. nspDBD Plasma Treatment atop an Acellular Barrier Impedes Component Diffusion

To investigate whether plasma components penetrate to affect ecto-CRT levels on tumor cells, we used a tissue model as a barrier and evaluated the cellular response in the monolayer below. Treatment at the same energy as that of the positive control resulted in a negligible increase to 7.8% from 7.5% ecto-CRT positive population (Fig. 3B). This suggests that plasma components generated at 300 mJ are unable to pass through the acellular barrier to influence the monolayer of cells, but, possibly, higher-energy plasma could. To assess whether CRT expression increased with increasing energy, the experiment was repeated with treatments at 700, 900, and 2000 mJ, which resulted in partial recovery even at the highest energy tested. Although this shows that plasma components penetrate further with higher energy, the energy required is too high to be safe for biological tissue.

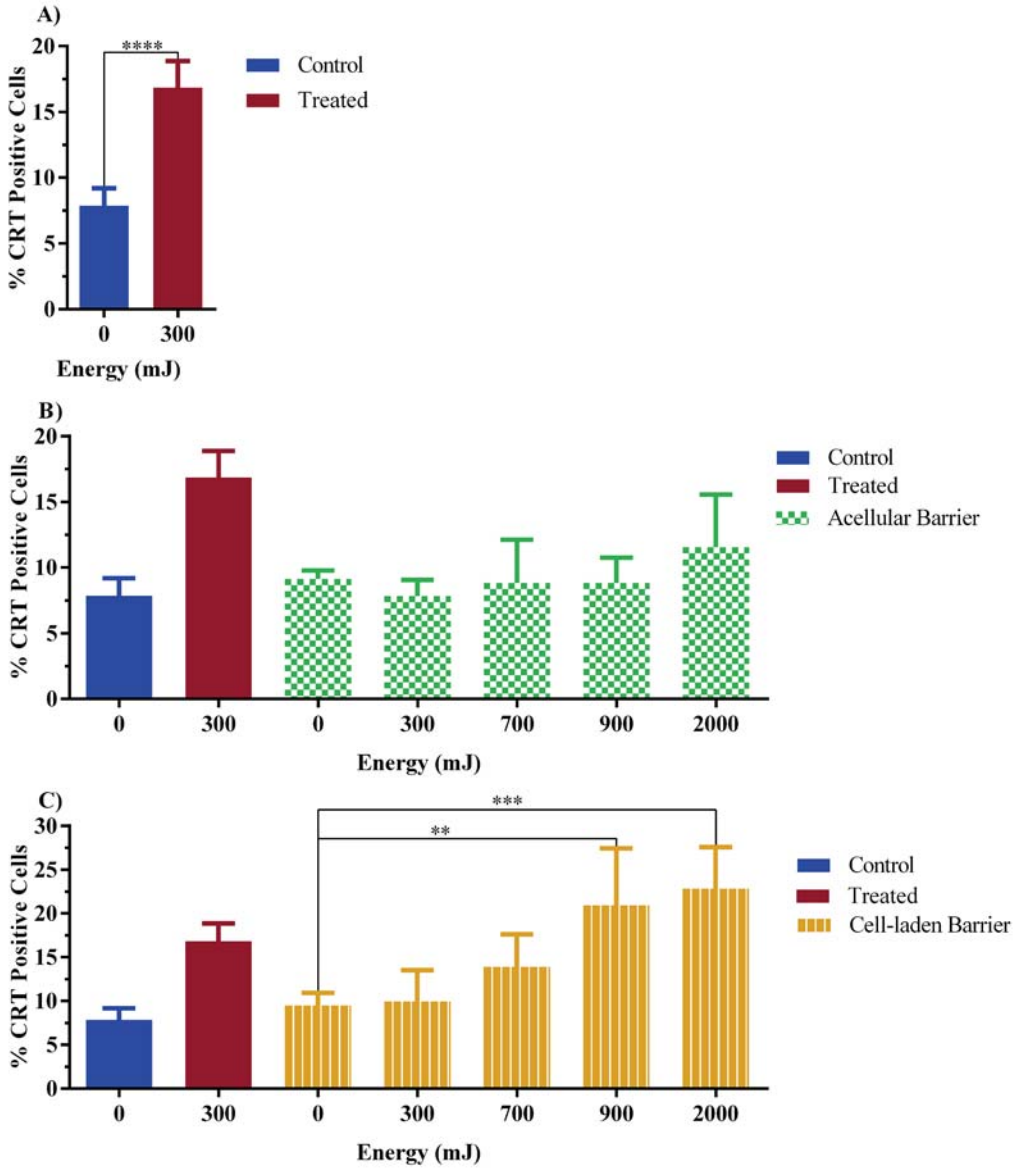

FIG. 3: nspDBD plasma penetrates through the tissue model to induce ecto-CRT expression in CT26 cells. ecto-CRT expression was measured 24 hr after plasma treatment. (A) Treatment of CT26 cells in the absence of a barrier doubles the expression of ecto-CRT. (B) Plasma generated atop an acellular 150-μm barrier abrogates the expression at lower energy. (C) With the addition of cells to the barrier, ecto-CRT expression in the target cells increases more than that that of the control at higher energy. Data are shown as the mean; error bars represent the standard error of the mean (SEM). The significance of the data was analyzed with the one-way ANOVA test, where $^{**}p < 0.01$, $^{***}p < 0.001$, and $^{****}p < 0.0001$.

C. Plasma-Stimulated Intercellular Signaling from the Barrier Increases Plasma Depth of Penetration

The externalization of CRT through the depth of the tumor has been documented in animal studies.[25,26] In other studies, *Drosophila* larvae treated with plasma exhibited an increase in fully differentiated hemocytes without any damage or change in physiology and life cycle.[27] This suggests that although plasma components may not penetrate, biological signaling may facilitate transfer of plasma effect. Therefore, we populated the barrier with cells to examine the influence of plasma-stimulated intercellular signaling on CRT induction in the target cells. The addition of cells to the barrier was expected to cause plasma components to interact with the embedded cells. Any effect on the target cells below would presumably be a result of cell-to-cell communication. Treatment atop the cell-laden barrier increased the percentage of cells with ecto-CRT expressed from 7.5% to 9.95% at 300 mJ. This indicates that the presence of cells enabled the plasma effect to travel to the target cells, but the effect was weak. The influence of this signaling is more evident with higher-energy plasma because the percentage of CRT-positive cells is higher at both 900 mJ (19.27%) and 2000 mJ (22.82%) than at the positive control (16.8%) (Fig. 3C). In comparison to the acellular barrier treated at the same plasma energies, the addition of cells to the barrier allowing for intercellular signaling resulted in higher ecto-CRT expression in the monolayer. In conclusion, plasma-stimulated intercellular signaling can increase the antitumor effects of plasma treatment.

D. nspDBD Plasma Treatment Induces Immediate ATP Release from Cells in the Barrier and Monolayer

Increased CRT expression in target cells showed that plasma might affect cells underneath the cell-laden barrier; however, the mechanism and plasma components responsible were still unclear. The typical reaction time for the expression of ecto-CRT in response to ICD inducers is a few hours after treatment, which is orders of magnitude longer than the lifetime of the plasma components.[2,28] Thus, to study the immediate direct effects of plasma treatment, we measured the extracellular ATP concentration. It was previously shown that nspDBD plasma causes cancer cells to release ATP within 10 min after treatment.[14] The concentration of extracellular ATP released in response to plasma treatment at 300 mJ was established in the monolayer. The amount of plasma treatment increased the measured ATP in extracellular fluid in untreated cells from 14 nM to 3.28 μM (Fig. 4A). With the addition of the acellular barrier and treatment at 2000 mJ, measured ATP was 1.84 μM, suggesting that the barrier impedes plasma components from penetrating target cells. Plasma treatment atop the cell-laden barrier at 2000 mJ resulted in an ATP value of 2.99 μM, comparable to the amount of ATP released with treatment of the monolayer. Although this seems to indicate that plasma-stimulated intercellular signaling can stimulate target cells to release more ATP (comparable to the positive control), this is not the case. When the cell-laden barrier was treated at 2000 mJ without target cells below, the measured ATP was 1.34 μM (Fig. 4A). This indicates that the cells embedded in the barrier contribute

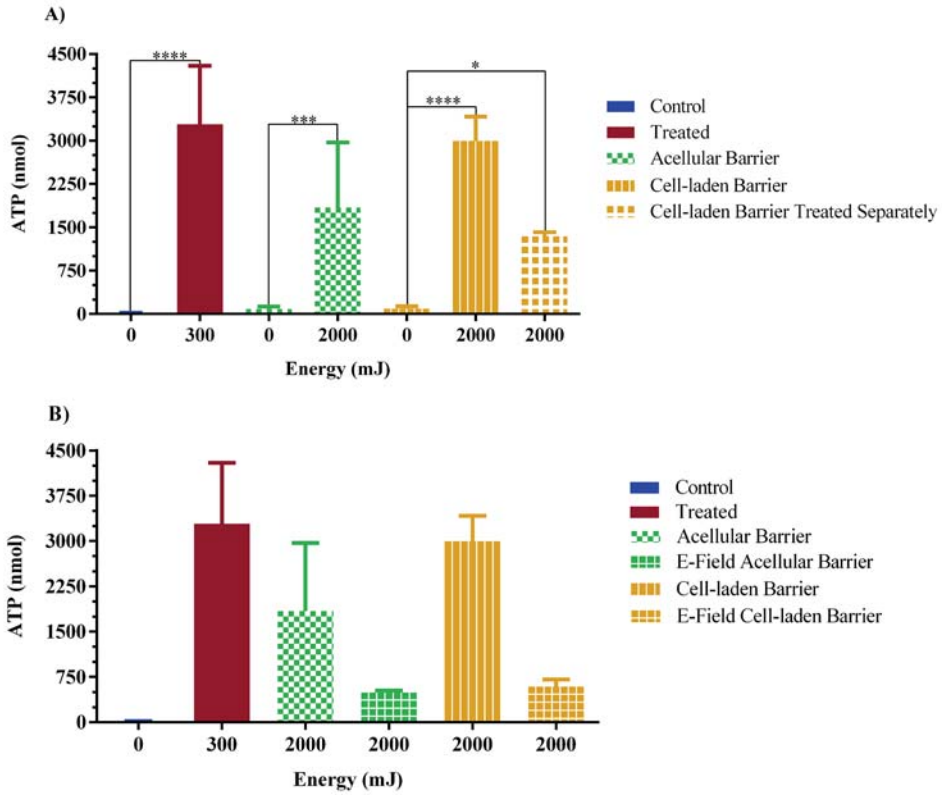

FIG. 4: Release of ATP in response to nspDBD plasma treatment through the tissue model. The concentration of extracellular ATP was measured 10 min after plasma treatment. (A) Treatment atop the acellular barrier attenuated the concentration of ATP released. The addition of cells to the barrier caused the overall concentration to increase; however, this is due to plasma treatment of the cells in the barrier rather than the increase of ATP release from the monolayer of cells. Thus, the cell signaling from the barrier does not increase the release of ATP from the target cancer cells. (B) Only the electric field was applied to the model to evaluate whether the nspEF caused direct effects of plasma. The ATP that was released due to the electric field was a fraction of the magnitude due to plasma. Data are shown as the mean; error bars represent the SEM. The significance of the data was analyzed with the one-way ANOVA, where $*p < 0.05$, $***p < 0.001$, and $****p < 0.0001$.

to the total measured ATP (2.99 μM) when evaluated in the presence of basal target cells. This shows that both the cells embedded in the barrier and the target cells react to plasma more quickly than the CRT response would indicate.

nsp electric fields (nspEFs), a component of nspDBD plasma, are theorized to assist in the penetration of tissue and disruption of cellular membranes.[29] To examine the influence of the nspEF of our system on the direct effects of plasma treatment, the gap distance between the barrier and electrode was filled with PBS without Ca and Mg, and

the nspEF was applied. The breakdown voltage for liquid is one order of magnitude higher than that for air; thus, only the electric field was applied.[30] The concentrations of ATP released were 491.5 and 589.8 nM for the acellular and cell-laden barrier, respectively (Fig. 4B). The nspEF-induced release of ATP was marginal in comparison to the concentration released in response to plasma. Although the ATP released originates from target cells in the acellular barrier case, it is indistinguishable whether cells in the barrier and/or target cells release ATP.

E. Transfer of Plasma-Induced CRT Expression Relies on Cell Proximity

For *in-vivo* xenograft models, the propagation distance of antitumor effects from the skin to the tumor below is further than the penetration depth of plasma-generated species.[11] This observation suggests a contribution of intercellular signaling. Signal transfer between two cells occurs after an activation of various factors from one cell to its neighbors (paracrine signaling) and/or through direct cell-to-cell contact signaling, such as occurs in gap junctions.[31] The cell-laden barrier data suggest that plasma components penetrate the tissue model and interact with cells within the barrier to stimulate subsequent signaling events. To assess whether paracrine signaling was the dominant signaling mechanism for inducing ecto-CRT expression in target cells, the cell-laden barrier was treated in a separate well before transfer, to prevent any immediate, direct contact with plasma components that could affect target cells. After the barrier was transferred to the monolayer and incubated for 24 hr, CRT expression was measured. The observed response in the CT26 cells was 11.49% at 2000 mJ (Fig. 5), which compares to the value of control without plasma treatment (10.65%). This indicates that paracrine signaling alone cannot sustain the transfer of effect and requires a close proximity between cells.

For the transfer of signals through direct contact, such as through gap junctions, the embedded cells should form connections with their cytoskeleton.[32] To examine whether this is the case, cell-laden barriers were fixed and stained for nucleic acid and the cytoskeleton to identify nuclei and cytoskeletal junctions, respectively. As shown in Fig. 6, the cytoskeleton surrounding the nuclei of the cells connects to form a network capable of signal propagation. Therefore, signal transfer through gap junctions could be a likely pathway in this tissue model and merits further investigation.

F. Calcium Wave Propagation

A proposed theory by Evans fits our model for the propagation of antitumor effects of plasma.[32] The mechanism of calcium-induced calcium release (CICR) requires both paracrine and direct contact signaling to propagate a wave of intracellular calcium among cells.[32–34] Studies have shown that plasma treatment of cancer cells increases intracellular calcium concentration.[35,36] Calcium can signal to nearby cells by inducing release of ATP or by itself being transferred through junctions to adjacent cells (Fig. 7). Released ATP degrades rapidly; thus, it will only signal to nearby cells. ATP binds to purinergic receptors on the cell membrane, which induces release of calcium from the endoplasmic

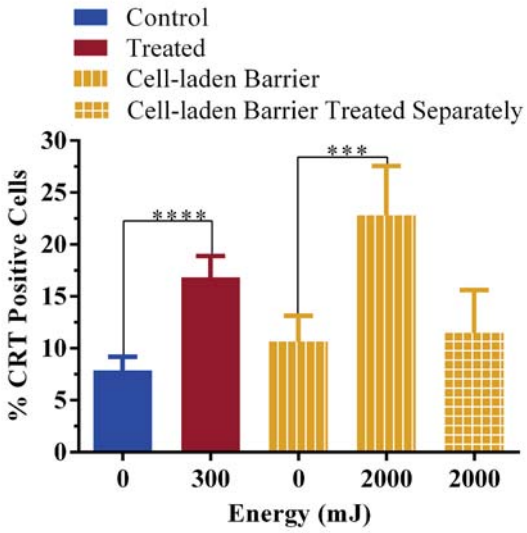

FIG. 5: Paracrine signaling affects plasma-induced ecto-CRT induction in CT26 cells. Cell-laden barriers were treated in a separate well and immediately transferred to a monolayer of CT26 cells. After incubating for 24 hr, ecto-CRT expression was measured in the monolayer. Removal of the direct contact between the tissue model and the monolayer during treatment reduced the effectiveness of nspDBD plasma to induce ecto-CRT in the monolayer. Data are shown as the mean; error bars represent the SEM. The significance of the data was analyzed with the one-way ANOVA test, where ***$p < 0.001$ and ****$p < 0.0001$.

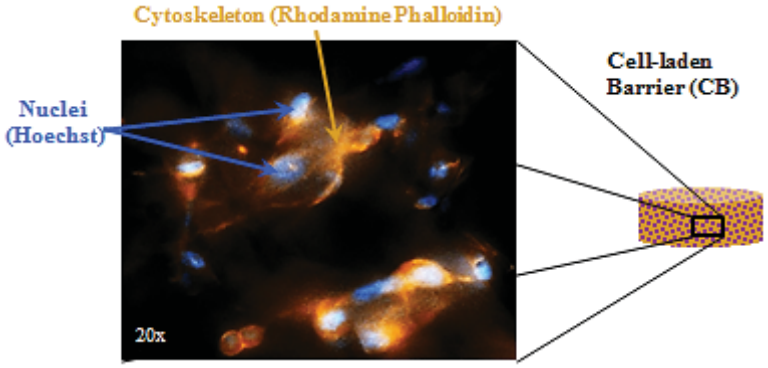

FIG. 6: CT26 cells in the barrier form junctions, enabling direct cell-to-cell signaling. After plasma treatment, cell-laden barriers were fixed in 4% PFA for 1 hr and washed with PBS without Ca and Mg. The barriers were permeabilized, blocked, and stained for nucleic acid and the cytoskeleton with Hoechst stain and phalloidin, respectively. The nuclei of the cells (blue, indicated by left-most arrows) were connected to one another through junctions of the cytoskeleton (orange, indicated by top-most arrow). The formation of junctions among cells in the barrier creates an intercellular network that allows cells to signal through direct contact, such as gap junctions.

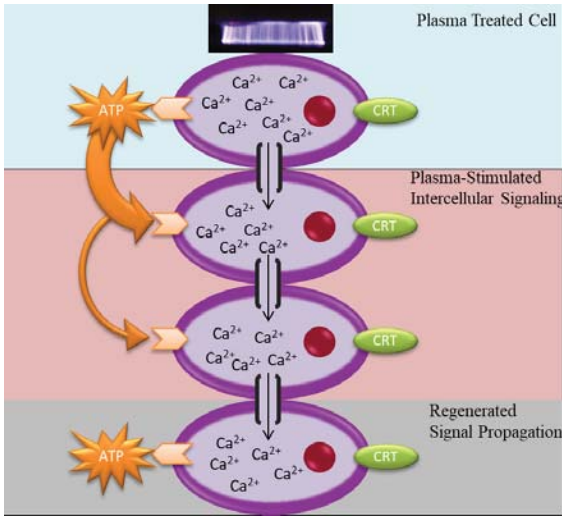

FIG. 7: CICR propagation of surface CRT expression. Plasma-induced calcium increase can be propagated from cell to cell via paracrine and direct contact signaling. The released ATP in response to plasma can signal nearby cells by binding to surface purinergic receptors, raising the calcium concentration. However, extracellular ATP rapidly degrades, limiting the propagation distance due to paracrine signaling. A calcium increase triggered in this way originates from the ER, where the depletion of ER calcium influences the expression of surface CRT. Calcium can travel as a wave among adjacent cells through direct contact signaling, reaching cells that cannot be influenced by ATP that is released as a result of plasma treatment. If the concentration is sufficient, these cells can further propagate the wave by calcium-induced release of ATP, thus regenerating the paracrine signaling propagation. Therefore, CICR propagation may be the mechanism for propagating plasma-stimulated effects.

reticulum (ER) and increases intracellular calcium concentration.[37] This supports our model, because the induction of surface CRT expression is favored when calcium in the ER is depleted.[38] When the concentration of extracellular ATP is insufficient to trigger ER calcium release, propagation due to paracrine signaling ceases. Excess calcium will also propagate as a wave among cells via gap junctions.[33] If the concentration of intracellular calcium is adequate, calcium can signal the release of ATP from cells that are not directly treated with plasma. Therefore, plasma treatment induces stress that can cause cells to propagate a gradient of intracellular calcium through CICR. This results in expression of surface CRT and release of ATP. We plan to test this hypothesis in future studies using inhibitors and signal blocking agents.

IV. CONCLUSION

This study reports on the enhanced propagation of plasma-stimulated antitumor effects through intercellular signaling in a tissue model. Indications of plasma treatment affect-

ing target tumor cells, expression of ecto-CRT, and release of ATP were higher in cancer cells beneath a cell-laden barrier than cells under an acellular barrier. This suggests that cells in the barrier responded to plasma treatment by enhancing the propagation of ICD-inducing factors to affect target cancer cells. Additionally, increasing plasma energy caused more of these factors (including both the components and intercellular signals) to reach the cells beneath the barriers, indicating that higher energies increase the depth of penetration of plasma treatment. Our future studies will address the maximum depth of penetration of individual plasma components and whether CICR is the signaling mechanism influencing the propagation. This will provide insight for the development of noninvasive cancer treatment that selectively affects tumor cells over healthy tissue and minimizes the potential for adverse side effects.

REFERENCES

1. Bauer G, Graves DB. Mechanisms of selective antitumor action of cold atmospheric plasma-derived reactive oxygen and nitrogen species. Plasma Proc Polymers. 2016;13:1157–78.
2. Graves DB. The emerging role of reactive oxygen and nitrogen species in redox biology and some implications for plasma applications to medicine and biology. J Phys D: Appl Phys. 2012;45(26):263001.
3. Panngom K, Baik KY, Ryu YH, Uhm HS, Choi EH. Differential responses of cancer cell lines to non-thermal plasma from dielectric barrier discharge. Curr Appl Phys. 2013;13:S6–11.
4. Schlegel J, Köritzer J, Boxhammer V. Plasma in cancer treatment. Clin Plasma Med. 2013;1(2):2–7.
5. Keidar M, Walk R, Shashurin A, Srinivasan P, Sandler A, Dasgupta S, Ravi R, Guerrero-Preston R, Trink B. Cold plasma selectivity and the possibility of a paradigm shift in cancer therapy. Br J Cancer. 2011;105(9):1295–301.
6. Vandamme M, Robert E, Pesnel S, Barbosa E, Dozias S, Sobilo J, Lerondel S, Le Pape A, Pouvesle JM. Antitumor effect of plasma treatment on U87 glioma xenografts: Preliminary results. Plasma Proc Polymers. 2010;7(3–4):264–73.
7. Utsumi F, Kajiyama H, Nakamura K, Tanaka H, Mizuno M, Ishikawa K, Kondo H, Kano H, Hori M, Kikkawa F. Effect of indirect nonequilibrium atmospheric pressure plasma on anti-proliferative activity against chronic chemo-resistant ovarian cancer cells in vitro and in vivo. PLoS ONE. 2013;8(12):e81576.
8. Fridman G, Shereshevsky A, Jost MM, Brooks AD, Fridman A, Gutsol A, Vasilets V, Friedman G. Floating electrode dielectric barrier discharge plasma in air promoting apoptotic behavior in melanoma skin cancer cell lines. Plasma Chem Plasma Proc. 2007;27(2):163–76.
9. Walk RM, Snyder JA, Srinivasan P, Kirsch J, Diaz SO, Blanco FC, Shashurin A, Keidar M, Sandler AD. Cold atmospheric plasma for the ablative treatment of neuroblastoma. J Ped Surg. 2013;48(1):67–73.
10. Guar N, Szili E, Oh J-S, Hong S-H, Michelmore A, Graves DB, Hatta A, Short RD. Combined effect of protein and oxygen on reactive oxygen and nitrogen species in the plasma treatment of tissue. Appl Phys Lett. 2015;107:6.
11. Partecke LI, Evert K, Haugk J, Doering F, Normann L, Diedrich S, Weiss F-U, Evert M, Huebner NO, Guenther C. Tissue tolerable plasma (TTP) induces apoptosis in pancreatic cancer cells in vitro and in vivo. BMC Cancer. 2012;12(1):473.
12. Graves DB. Reactive species from cold atmospheric plasma: Implications for cancer therapy. Plasma Proc Polymers. 2014;11(12):1120–7.
13. Miller V, Lin A, Fridman A. Why target immune cells for plasma treatment. Plasma Chem Plasma Proc. 2016;36(1):259–68.
14. Lin A, Truong B, Pappas A, Kirifides L, Oubarri A, Chen S, Lin S, Dobrynin D, Fridman G, Fridman A. Uniform nanosecond pulsed dielectric barrier discharge plasma enhances anti-tumor effects by in-

duction of immunogenic cell death in tumors and stimulation of macrophages. Plasma Proc Polymers. 2015;12(12):1392–9.
15. Koks CA, Garg AD, Ehrhardt M, Riva M, Vandenberk L, Boon L, Vleeschouwer SD, Agostinis P, Graf N, Van Gool SW. Newcastle disease virotherapy induces long-term survival and tumor-specific immune memory in orthotopic glioma through the induction of immunogenic cell death. Int J Cancer. 2015;136(5):E313–25.
16. Witek M, Blomain ES, Magee MS, Xiang B, Waldman SA, Snook AE. Tumor radiation therapy creates therapeutic vaccine responses to the colorectal cancer antigen GUCY2C. Int J Radiat Oncol Biol Phys. 2014;88(5):1188–95.
17. Miller V, Lin A, Fridman G, Dobrynin D, Fridman A. Plasma stimulation of migration of macrophages. Plasma Proc Polymers. 2014;11(12):1193–7.
18. Kaushik NK, Kaushik N, Min B, Choi KH, Hong YJ, Miller V, Fridman A, Choi EH. Cytotoxic macrophage-released tumor necrosis factor-alpha (TNF-α) as a killing mechanism for cancer cell death after cold plasma activation. J Phys D: Appl Phys. 2016;49(8):1–20.
19. Lin A, Xiang B, Snook AE, Fridman G, Fridman A, Miller V. Non-thermal plasma induction of immunogenic cell death in an in-vivo tumor mouse model. ICPM-6: Proceedings of the 6th International Conference on Plasma Medicine; 2016 Sep 4–9; Bratislava, Slovakia.
20. Han L-H, Yu S, Wang T, Behn A, Yang F. Microribbon-like elastomers for fabricating macroporous and highly flexible scaffolds that support cell proliferation in 3D. Adv Func Mater. 2013;23:346–58.
21. Han L-H, Tong X, Fan Y. Photo-crosslinkable PEG-based microribbons for forming 3D macroporous scaffolds with decoupled niche properties. Adv Mater. 2014;26:1757–62.
22. Garg AD, Krysko DV, Verfaillie T, Kaczmarek A, Ferreira GB, Marysael T, Rubio N, Firczuk M, Mathieu C, Roebroek AJ. A novel pathway combining calreticulin exposure and ATP secretion in immunogenic cancer cell death. EMBO J. 2012;31(5):1062–79.
23. Masur K, Von Behr M, Bekeschus S, Weltmann KD, Hackbarth C, Heidecke C-D, Von Bernstorff W, Von Woedtke T, Partecke LI. Synergistic inhibition of tumor cell proliferation by cold plasma and gemcitabine. Plasma Proc Polymers. 2015;12:1377–82.
24. Bekeschus S, Von Woedtke T, Kramer A, Weltmann KD, Masur K. Cold physical plasma treatment alters redox balance in human immune cells. Plasma Med. 2013;3(4):267–78.
25. Lin A, Snook AE, Fridman A, Fridman G, Ownbey R, Truong B, Miller V. Non-thermal plasma application for cancer immunotherapy. IWPCT: Proceedings of the 3rd International Workshop on Plasma for Cancer Treatment; 2016 Apr 11–12; Washington, D.C.
26. Miller V, Lin A, Gururaja Rao S, Ownbey R, Snook AE, Fridman A, editors. Plasma activation of the immune system. ISPC 22: Proceedings of the 22nd International Symposium on Plasma Chemistry; 2015 July 5–10; Antwerp, Belgium.
27. Lee A, Lin A, Shah K, Singh H, Miller V, Rao SG. Optimization of non-thermal plasma in an in vivo model organism. PLoS ONE. 2016;11(8):e0160676.
28. Panaretakis T, Kepp O, Brockmeier U, Tesniere A, Bjorklund AC, Chapman DC, Durchschlag M, Joza N, Pierron G, van Endert P. Mechanisms of pre-apoptotic calreticulin exposure in immunogenic cell death. EMBO J. 2009;28(5):578–90.
29. Steuer A, Schmidt A, Laboha P, Babica P, Kolb JF. Transient suppression of gap junctional intercellular communication after exposure to 100-nanosecond pulsed electric fields. Bioelectrochemistry. 2016;112:33–46.
30. Lin A, Chernets N, Han J, Alicea Y, Dobrynin D, Fridman G, Freeman TA, Fridman A, Miller V. Nonequilibrium dielectric barrier discharge treatment of mesenchymal stem cells: Charges and reactive oxygen species play the major role in cell death. Plasma Proc Polymers. 2015;12(10):1117–27.
31. Bloemendal S, Kuck U. Cell-to-cell communication in plants, animals and fungi: A comparative review. Sci Nat Naturwissenschaften. 2013;100:3–19.
32. Evans WH. Cell communication across gap junctions: A historical perspective and current developments. Biochem Soc Trans. 2015;43:450–9.

33. Goldberg M, De Pittà M, Volman V, Berry H, Ben-Jacob E. Nonlinear gap junctions enable long-distance propagation of pulsating calcium waves in astrocyte networks. PLoS Comput Biol. 2010;6(8):e1000909.
34. Hajnóczky G, Davies E, Madesh M. Calcium signaling and apoptosis. Biochem Biophys Res Comm. 2003;304(3):445–54.
35. Dobrynin D, Fridman G, Friedman G, Fridman A. Physical and biological mechanisms of direct plasma interaction with living tissue. New J Phys. 2009;11(11):115020.
36. Sasaki S, Kanzaki M, Kaneko T. Calcium influx through TRP channels induced by short-lived reactive species in plasma-irradiated solution. Sci Rep. 2016;6:25728.
37. Vénéreau E, Ceriotti C, Bianchi ME. DAMPs from cell death to new life. Front Immunol. 2015;6:422.
38. Tufi R, Panaretakis T, Bianchi K, Criollo A, Fazi B, Di Sano F, Tesniere A, Kepp O, Paterlini-Brechot P, Zitvogel L, Piacentini M, Szabadkai G, Kroemer G. Reduction of enoplasmic reticulum Ca^{2+} level favors plasma membrane surface exposure of calreticulin. Cell Death Differen. 2008;15:274–82.